The Architecture of Cognitive Control in the Human Prefrontal Cortex

Etienne Koechlin,[1]* Chrystèle Ody,[1] Frédérique Kouneiher[2]

The prefrontal cortex (PFC) subserves cognitive control: the ability to coordinate thoughts or actions in relation with internal goals. Its functional architecture, however, remains poorly understood. Using brain imaging in humans, we showed that the lateral PFC is organized as a cascade of executive processes from premotor to anterior PFC regions that control behavior according to stimuli, the present perceptual context, and the temporal episode in which stimuli occur, respectively. The results support an unified modular model of cognitive control that describes the overall functional organization of the human lateral PFC and has basic methodological and theoretical implications.

Cognitive control, the ability to coordinate thoughts and actions in relation with internal goals, is often required in our everyday life and subserves higher cognition processes such as planning and reasoning. Cognitive control primarily involves the lateral prefrontal cortex (LPFC) (*1*–*4*) and exerts its influence through top-down interactions between LPFC regions and premotor or posterior associative cortices. The functional organization of the LPFC and the related cognitive architecture underlying cognitive control remain, however, poorly understood. No converging view has emerged yet from previous studies that have often reported inconsistent or elusive functional divisions within the LPFC (*5*, *6*).

A cascade model of cognitive control. To understand the architecture of cognitive control in the LPFC, we proposed a modular model postulating that the LPFC is organized as a hierarchy of representations originating from the premotor cortex (*3*) and processing distinct signals involved in controlling the selection of appropriate stimulus-response associations (*2*, *4*, *7*). The key assumption is the distinction between control processes operating with respect to either the perceptual context or the temporal episode in which the person is acting. Recent psychological models have proposed a similar distinction between executive processes involved in perceptual and episodic domains (*8*).

Specifically, we hypothesized that cognitive control involves at least three nested levels of processing, implemented in distinct frontal regions (Fig. 1). First, sensory control involved in selecting motor actions in response to stimuli and subserved by lateral premotor regions. Second, contextual control subserved by caudal LPFC regions [typically, Brodman's area (BA) 9/44/45] and involved in selecting premotor representations (that is, stimulus-response associations) according to external contextual signals accompanying stimulus occurrences. Third, episodic control subserved by rostral LPFC regions (typically BA 46) and involved in selecting caudal LPFC representations (task sets or consistent sets of stimulus-response associations evoked in the same context) according to the temporal episode in which stimuli occur; that is, according to events that previously occurred or to ongoing internal goals. The three processing levels are assumed to receive information about stimuli, contexts, and episodes from posterior associative areas. In agreement with the network of anatomical connections previously described in the frontal lobes (*9*), the model especially assumes a cascade of top-down controls from rostral to caudal LPFC and premotor regions.

As previously suggested (*10*), we assumed that cognitive control varies as the information (Shannon's information in the sense of information theory) conveyed by control signals and required for selecting appropriate representations for action. Accordingly, episodic control was assumed to vary as the information I_{cues} conveyed by episodic signals (past events) and required for selecting task sets, when stimuli and contextual signals occur. Similarly, contextual control was assumed to vary as the information I_{cont} conveyed by contextual signals about task sets, when stimuli occur. Sensory control was assumed to vary as the information I_{stim} conveyed by stimuli about motor responses. The cascade model then predicts, on the basis of information theory [see (*11*) for the underlying mathematical model], that episodic, contextual, and sensory controls make cumulative contributions to cognitive control that gradually sum up from rostral to caudal LPFC and premotor regions.

The cascade model predicts that the increasing demands of sensory, contextual, and episodic controls have additive effects on behavioral reaction times (*12*). Moreover, assuming that local brain activations as measured by functional magnetic resonance imaging (fMRI) vary as the amount of locally processed information, the increasing demands of sensory, contextual, and episodic controls are predicted to have additive cumulative effects on local fMRI activations that sum up from rostral to caudal LPFC and premotor regions.

Experimental paradigm. The model was tested by scanning 12 healthy people in two behavioral experiments designed to separately vary the demands of sensory, contextual, and episodic control (I_{stim}, I_{cont}, and I_{cues}, respectively). In both experiments, participants responded to series of successively presented visual stimuli broken down into successive blocks (behavioral episodes) preceded by distinct instruction cues (episodic signals). The demands of sensory, contextual, and episodic control were varied by manipulating three experimental factors: the stimulus, context, and episode factors, respectively (fig. S1) (*11*).

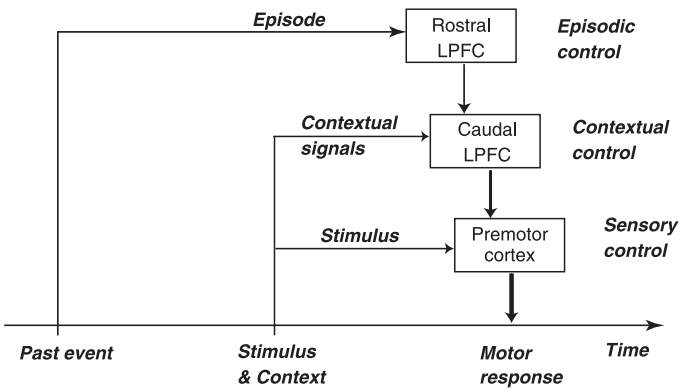

Fig. 1. The functional model.

[1]Institut National de la Santé et de Recherche Médicale, Université Pierre et Marie Curie, 9, quai St Bernard, 75005 Paris, France. [2]Hôpital Pitié-Salpêtrière, 47 boulevard de l'Hôpital, 75013 Paris, France.

*To whom correspondence should be addressed. E-mail: koechlin@ccr.jussieu.fr

In the motor experiment, we employed a factorial block design crossing the stimulus and episode factors (*11*). No contextual signal was used, so that no contextual control occurred. The stimulus factor contrasted one-forced-response episodes (detection task, $I_{stim} = 0$ bit) and two-forced-responses episodes (discrimination task, $I_{stim} = 1$ bit). The episode factor was the covariate that contrasted episodes according to the information I_{cues} conveyed by instruction cues and required for subsequently selecting appropriate stimulus-response associations ($I_{cues} = 0$ to 1 and 2 bit).

In the task experiment, we employed a factorial block design crossing the context and episode factors (*11*). Participants responded to stimuli by performing discrimination tasks, so that only two-forced-responses episodes were included (sensory control was maintained constant). Task sets to be performed depended on visually presented contextual signals accompanying stimulus occurrences. The context factor contrasted single-task-set episodes (single-task performance regardless of contextual signals, $I_{cont} = 0$ bit) and dual-task-set episodes (dual-task performance depending on contextual signals, $I_{cont} = 1$ bit). Again, the episode factor was the covariate that contrasted episodes according to the information I_{cues} conveyed by instruction cues and required for subsequently selecting appropriate task sets with respect to contextual signals ($I_{cues} = 0$ to 1 and 2 bit)

From the cascade model, we then predicted that rostral and caudal LPFC and premotor regions would exhibit effects of episode. Effects of context were expected in the caudal LPFC and premotor regions, whereas effects of stimulus were expected in premotor regions only. In each region, all effects were predicted to be additive. Furthermore, in rostral LPFC regions, the effect of episode was expected to be the same in both experiments. In contrast, in caudal LPFC regions, the effect of episode was expected to be steeper in the task than in the motor experiment, because in the task experiment those regions were predicted to engage episodic control for selecting task sets, whereas in the motor experiment those regions were predicted to simply convey top-down episodic control to premotor regions for selecting stimulus-response associations. In premotor regions, in contrast, the effects of episode were predicted to be the same, because in both experiments, selecting stimulus-response associations was assumed to engage top-down control from caudal LPFC regions. Consequently, the resulting effect of episode on reaction times was expected to be steeper in the task than in the motor experiment.

Frontal organization of cognitive control. Mean reaction times (RTs) significantly increased with the stimulus ($F = 90.5$, $P < 0.001$), context ($F = 85.9$, $P < 0.001$), and episode ($F = 297.1$, $P < 0.001$) factors (Fig. 2) (*11*). As predicted, the effects of stimulus and context were additive with the episode effect (interaction, both F's < 1.8, $P > 0.2$). The episode effect was significantly steeper in the task than in the motor experiment (interaction, $F = 27.2$, $P < 0.001$). Comparing RTs in the first and second half of episodes, we found that no effect significantly varied over episodes (all interactions, $F < 2.96$, $P > 0.11$), indicating that episodic control was not restricted to selecting instructions at episode onsets but was recurrently exerted in all subsequent trials.

fMRI data confirmed the implementation of the cascade model in the frontal lobes (Fig. 3) (*11*). Frontal regions exhibiting an effect of stimulus were found in the premotor cortex bilaterally (BA 6, middle frontal gyrus), whereas frontal regions showing an effect of context but no stimulus effect were observed in caudal LPFC bilaterally (BA 44/45, inferior frontal gyrus). Frontal regions exhibiting an effect of episode but no stimulus or context effects were found in rostral LPFC bilaterally (BA 46, inferior/middle frontal gyrus). No additional frontal regions were found when the episode effect was separately computed in each experiment. Outside the frontal lobes, effects of stimulus, context, and episode were especially found in posterior associative areas (table S1).

Analyses of covariance performed on activations identified above confirmed the model predictions (*11*). In rostral LPFC regions, mean activations linearly varied as the episode factor only (main effect, $F = 112.7$, $P < 0.001$) independently of hemisphere (left verus right, $F < 3.1$, $P > 0.11$) and regardless of experiment, stimulus, and context factors (all interactions, $F < 1.8$, $P > 0.21$) (Fig. 4A). No other effects or interactions were significant.

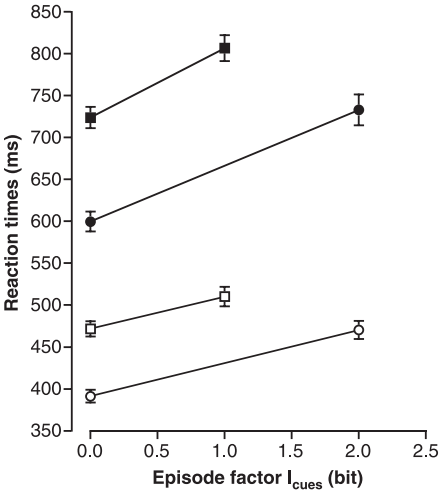

Fig. 2. Behavioral results. Reaction times to stimuli (mean ± SE across participants averaged over correct responses) across experimental conditions. Open circles and squares indicate one-forced-response and two-forced-response episodes, respectively (motor experiment). Solid circles and squares indicate single-task-set and dual-task-set episodes, respectively (task experiment). In all conditions, the participant's error rates were lower than 3% and exhibited no significant effect of stimulus, context, and episode.

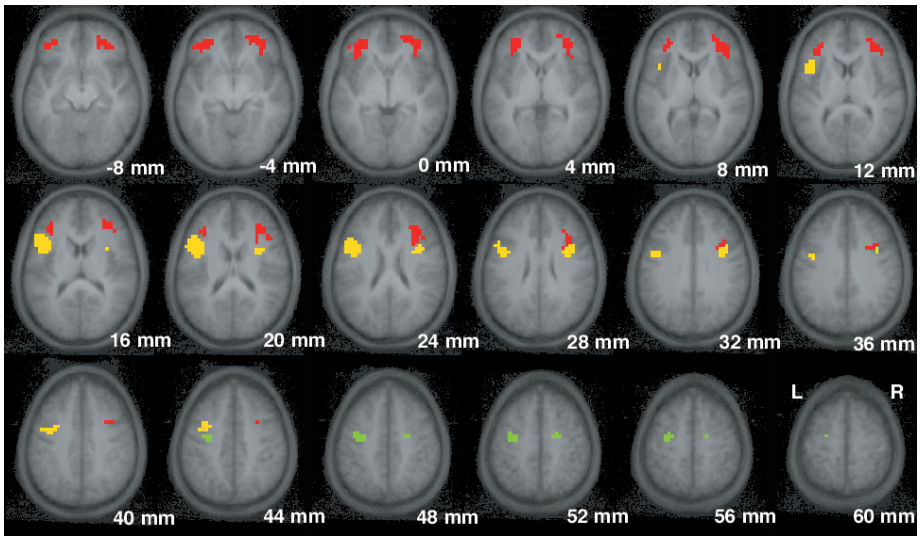

Fig. 3. Topography of brain activations. Green: Regions exhibited a stimulus effect (Talairach coordinates of maximal fixed-effect Z scores: $x,y,z = -32,-8, 56$ and $20, -8, 52$, $Z_{max} = 6.6$ and 5.1). Yellow: Regions exhibited a context effect but no stimulus effect ($x,y,z = -44, 8, 20$ and $36, 8, 28$, $Z_{max} = 8.9$ and 6.2). Red: Regions showing an episode effect but no stimulus and context effect ($x,y,z = -40, 32, 20$ and $=32, 32, 20$, $Z_{max} = 9.0$ and 17.3). Activations are superimposed on anatomical axial slices averaged across participants (neurological convention) and indexed by the vertical Talairach coordinate (z). All reported activations exhibited significant effects in fixed-effect ($Z > 4.3$, $P < 0.05$ corrected for multiple comparisons) and in subsequent random-effect ($P < 0.05$, corrected for multiple comparisons over the search volumes) analyses. The stimulus effect was computed as larger activations in two-forced-choice than one-forced-choice episodes with $I_{cues} = 0$, the context effect as larger activations in dual-task-set than single-task-set episodes with $I_{cues} = 0$, and the episode effect as activations linearly varying as I_{cues}.

Bilateral caudal LPFC regions exhibited a main effect of context and episode (both F's $>$ 48.7, P's $<$ 0.001) (Fig. 4, B and C). The two effects were additive (interaction, $F < 1.5$, $P > 0.23$, task experiment) and independent of hemisphere (both F's < 1). No stimulus effects (main effect and interactions) were observed (all F's < 3.3, $P > 0.10$ except for the interaction between the stimulus and context factors: $F = 26.8$, $P < 0.001$). The effect of episode was steeper in the task than in the motor experiment (interaction, $F = 16.5$, $P < 0.001$).

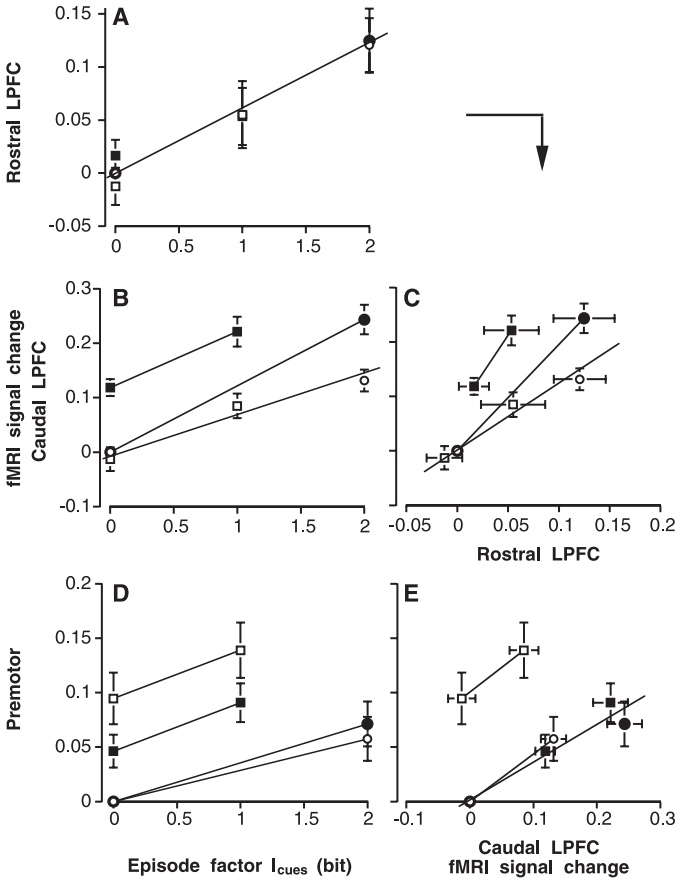

Fig. 4. Factorial analyses of regional activations. Mean activations computed over each region (averaged regression coefficients relative to baseline ± SEs across participants) are plotted against the episode factor I_{cues} (left panels) and the mean activations of regions that exert top-down control according to the model (right panels). Left and right activations are averaged together. The baseline is the one-forced-response condition (motor experiment) and the single-task-set condition (task experiment) with $I_{cues} = 0$. (**A**) Rostral LPFC. (**B** and **C**) Caudal LPFC. (**D** and **E**) Premotor regions. See Fig. 3 for graph legends.

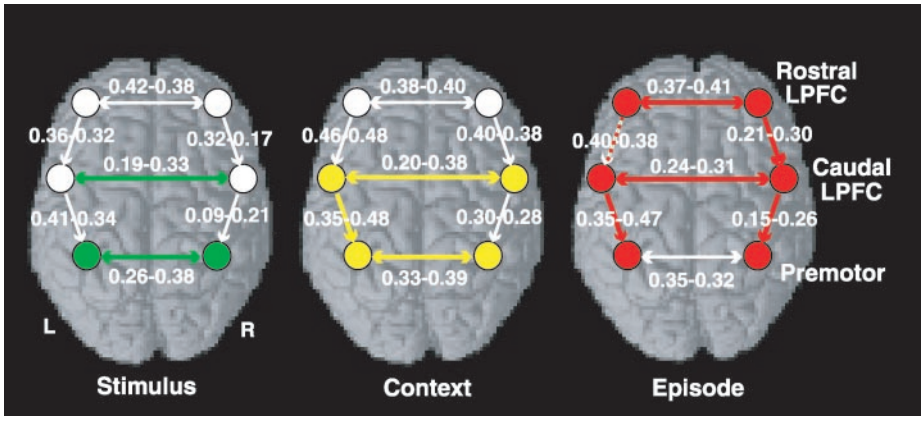

Fig. 5. Diagram of effective connectivity. Structural equation modeling included oriented structural paths (arrows) connecting frontal regions (circles, neurological convention, approximate locations) described in the text. L, left; R, right. (**Left**) Path coefficients in one-forced-response (left number) and two-forced-response (right number) episodes (motor experiment). (**Middle**) Path coefficients in single-task-set (left number) and dual-task-set (right number) episodes (task experiment). (**Right**) Path coefficients in episodes (both experiments) associated with $I_{cues} = 0$ (left number) and $I_{cues} > 0$ (right number). Frontal activations and path coefficients that significantly increased with the stimulus, context, and episode factors are shown in green, yellow, and red, respectively. The red dashed arrow in the right panel indicates a path coefficient that over both experiments did not significantly vary with the episode factor but significantly increased in the task experiment (0.40 to 0.53, $\chi^2 = 12.1$, $P < 0.001$) and significantly decreased in the motor experiment (0.39 to 0.29, $\chi^2 = 4.5$, $P < 0.035$).

Bilateral premotor regions exhibited a main effect of stimulus, context, and episode (all F's > 17.3, $P < 0.001$) regardless of hemisphere (all F's < 1) (Fig. 4, D and E). The main effect of episode was independent of experiment ($F < 1$) and additive with both the stimulus and context factors (both interactions, F's < 1.8, $P > 0.20$).

Effective connectivity in the frontal lobes. Finally, we explicitly tested the model prediction that the effects of episode and context observed in caudal LPFC and premotor regions result from top-down control from rostral to caudal LPFC and premotor regions. The functional model was therefore reformulated as a model of structural linear equations with path coefficients quantifying effective connectivity as partial temporal correlations between related regional activations (*11*, *13*, *14*). In addition to top-down paths from rostral to caudal and premotor regions, the structural equation model included additional reciprocal paths linking the same regions located in the left and right hemispheres to account for callosal interhemispheric connections. Variations of effective connectivity or path coefficients were then estimated with respect to each experimental factor by computing interregional correlation matrices for each factor level (Fig. 5).

Because the model assumes that episodic control is exerted from rostral to caudal LPFC and premotor regions, path coefficients increasing with the episode factor were expected to connect rostral LPFC to premotor regions. Significantly increasing path coefficients were found between left and right rostral LPFC regions and from rostral to caudal right LPFC regions (both χ^2s > 5.3, $P < 0.02$), between left and right caudal LPFC regions, and bilaterally from caudal LPFC to premotor regions (all χ^2s > 8.2, $P < 0.004$) (Fig. 5). The same pattern was observed in both experiments [except the path coefficient from rostral to caudal left LPFC regions (Fig. 5)]. The same results were found even when the model included additional path coefficients directly connecting rostral LPFC to premotor regions. Those direct path coefficients decreased when the episode factor increased, even in the motor experiment, indicating that information flows related to episodic control exerted by the rostral LPFC on premotor regions involved caudal LPFC regions.

Similarly, because the model assumes that contextual control is exerted from caudal LPFC to premotor regions, path coefficients increasing with the context factor were expected to connect caudal LPFC to premotor regions. Significantly increasing path coefficients were found only between left and right caudal LPFC regions, from left caudal LPFC to left premotor regions (both χ^2s > 12.7, $P < 0.001$), and between left and right premotor regions ($\chi^2 = 4.8$, $P = 0.03$) (Fig. 5).

In contrast, the model predicts that sensory control involves no top-down control from

prefrontal regions. Path coefficients that significantly increased with the stimulus factor were found only between left and right premotor regions and between left and right caudal LPFC regions (both χ^2s > 20.5, $P < 0.001$; other coefficients, $\chi^2 < 2.3$, $P > 0.16$) (Fig. 5). This finding is consistent with the fact that the stimulus factor contrasted one-forced-response with two-forced-response episodes, including unilateral (left or right) versus bilateral responses, respectively.

A unified modular theory of lateral prefrontal functions. These results rule out the possibility that activations observed in the caudal and rostral LPFC result from increases in mental effort alone, because the greatest caudal and rostral LPFC activations were found when episodic control was maximal but not when behavioral performances were the most degraded (Figs. 2 and 4) (*15*).

Additionally, rostral LPFC activations are unlikely to result from variations in working memory load (*16*) (that is, from maintaining instructions related to cues over subsequent episodes) and from variations in relational complexity (*17*) across conditions. Indeed, in these two alternative interpretations, because memory load and relational complexity were larger in dual-task-set than in single-task-set episodes (memory load was also larger in two-forced-response than in one-forced-response episodes), an effect of context (and of stimulus for memory load) should have been observed in rostral LPFC regions. In both experiments, however, rostral LPFC activations varied as the episode factor only.

Time courses of rostral LPFC activations (fig. S2) and behavioral data also revealed that the episode effect was sustained over episodes, so that regardless of working memory load and relational complexity, rostral LPFC regions are engaged for recurrently selecting appropriate representations for action selection over episodes after the occurrences of behaviorally significant events. Furthermore, rostral LPFC regions exert control on the caudal LPFC but not directly on premotor representations, because caudal LPFC activations and the effective connectivity between rostral and caudal LPFC activations increased with the episode factor, whereas effective connectivity between rostral LPFC and premotor regions did not (Figs. 4 and 5). Control is exerted from rostral to caudal rather than from caudal to rostral LPFC regions, because caudal LPFC regions exhibited a context effect that was not observed in rostral LPFC regions.

In the task experiment, the context effect observed in caudal LPFC regions is consistent with at least two interpretations. It may result from the engagement of caudal LPFC regions in selecting task sets according to contextual signals or simply in maintaining task sets in working memory over episodes. However, the working memory interpretation alone does not account for the episode effect observed in those regions, because in the task experiment the episode factor varied frequencies of associations between contextual signals and task sets, whereas frequencies of tasksets alone were maintained constant across conditions. Rostral LPFC regions thus select caudal LPFC representations associating contextual signals and task sets and mediating the selection of task sets with respect to contextual signals. This conclusion is supported by the flatter effect of episode observed in the motor experiment, when no contextual signals were presented.

The combined effects of stimulus and episode observed in premotor and caudal LPFC regions in the motor experiment were virtually identical to the combined effects of context and episode found in caudal and rostral LPFC regions in the task experiment (Fig. 4). We concluded that caudal LPFC regions select premotor representations associating stimulus and motor responses and mediating the selection of motor responses with respect to stimuli. In the task experiment, the effects of context and episode observed in premotor regions simply reflected the top-down control that caudal LPFC regions exert on premotor regions (Figs. 4E and 5). Top-down effects exerted on premotor regions were the same in both experiments (Fig. 4E), in agreement with the involvement of top-down signals in selecting appropriate stimulus-response associations in both experiments.

Our findings explain the pattern of prefrontal activations observed in several experimental paradigms, including learning (*18*, *19*), episodic memory (*20*), working memory (*21*), and task-switching (*22*–*25*) paradigms. Consistent with our model, in all these paradigms, caudal and rostral LPFC activations were observed, depending on whether the executive control of behavior was based on contextual or episodic signals (supporting online text).

In particular, we showed that episodic control involves rostral LPFC regions, indicating that rostral LPFC activations crucially depend on the amount of interference and cross-talk that may occur between instructions given to participants in different experimental episodes. Rostral LPFC regions thus represent ongoing episodes or plans involving specific behavioral rules. This finding is consistent with previous studies showing that more anterior prefrontal regions located in the frontopolar cortex are selectively involved in cognitive branching; that is, in processes controling the activation of subepisodes nested in ongoing behavioral episodes, with some evidence that those regions exert control on rostral LPFC representations (*25*, *26*). Thus, the cascade model may be extended to frontopolar regions and to branching control exerted on rostral LPFC representations.

We showed that the human lateral frontal cortex is functionally organized as a cascade of control processes mediating sensory, contextual, and episodic control implemented in premotor regions and in caudal and rostral LPFC regions, respectively. The cascade model combines the views that the prefrontal cortex is organized as a hierarchy of processing mediating the temporal organization (*3*, *27*) and the cognitive control (*2*, *28*) of behavior. The cascade model generalizes the classical theory of executive control based on a central executive system controlling multiple maintenance slave systems (*29*) to a multistage cascade architecture. Each stage maintains active representations that are controlled by higher stages and that exert control on representations in lower stages. In this architecture, we showed that the engagement of prefrontal regions along the posteroanterior axis is not primary based on the relational complexity or memory load but on the temporal structure of representations underlying executive control.

Our results revealed that frontal activations as well as participants' reaction times linearly varied as Shannon's information conveyed by episodic signals given other external signals; that is, as the logarithm of the inverse frequency that behavior was based on congruent associative representations across behavioral episodes. This finding is consistent with the additive effects of sensory, contextual, and episodic controls observed in frontal regions. Shannon's information conveyed by external control signals about action selection thus provides a computational and causal account for the psychological concept of cognitive control related to those signals (*10*). Cognitive control then appears to be governed by psychophysical laws that are formally similar to Weber-Fechner laws underlying human perception (*30*, *31*), suggesting that information processing underlying cognitive control and perception may obey common basic principles of neuronal computations.

References and Notes

1. P. C. Fletcher, R. N. Henson, *Brain* **124**, 849 (2001).
2. E. K. Miller, J. D. Cohen, *Annu. Rev. Neurosci.* **24**, 167 (2001).
3. J. M. Fuster, *The Prefrontal Cortex. Anatomy, Physiology, and Neuropsychology of the Frontal Lobe* (Raven, New York, ed. 2, 1989).
4. T. Shallice, P. Burgess, *Philos. Trans. R. Soc. London Ser. B* **351**, 1405 (1996).
5. J. Duncan, A. M. Owen, *Trends Neurosci.* **23**, 475 (2000).
6. J. N. Wood, J. Grafman, *Nature Rev. Neurosci.* **4**, 139 (2003).
7. R. E. Passingham, *The Frontal lobes and Voluntary Action* (Oxford Psychology Series, Oxford Univ. Press, Oxford, 1993).
8. A. Baddeley, *Trends Cogn. Sci.* **4**, 417 (2000).
9. D. N. Pandya, E. H. Yeterian, in *Neurobiology of Decision-Making*, A. R. Damasio, H. Damasio, Y. Christen, Eds. (Springer-Verlag, Berlin, 1996), pp. 13–46.
10. D. E. Berlyne, *Psychol. Rev.* **64**, 329 (1957).
11. Materials and methods are available as supporting material on *Science* Online.
12. S. Sternberg, *Acta Psychol.* **30**, 276 (1969).
13. A. R. McIntosh, F. Gonzalez-Lima, *Hum. Brain Mapp.* **2**, 2 (1994).

14. K. J. Friston, C. D. Frith, R. S. J. Frackowiak, *Hum. Brain Mapp.* **1**, 69 (1993).
15. M. L. Furey *et al.*, *Proc. Natl. Acad. Sci. U.S.A.* **94**, 6512 (1997).
16. D. J. Veltman, S. A. Rombouts, R. J. Dolan, *Neuroimage* **18**, 247 (2003).
17. K. Christoff *et al.*, *Neuroimage* **14**, 1136 (2001).
18. I. H. Jenkins, D. J. Brooks, P. D. Nixon, R. S. Frackowiak, R. E. Passingham, *J. Neurosci.* **14**, 3775 (1994).
19. E. Koechlin, A. Danek, Y. Burnod, J. Grafman, *Neuron* **35**, 371 (2002).
20. R. L. Buckner, W. Koutstaal, *Proc. Natl. Acad. Sci. U.S.A.* **95**, 891 (1998).
21. J. B. Rowe, I. Toni, O. Josephs, R. S. Frackowiak, R. E. Passingham, *Science* **288**, 1656 (2000).
22. A. Dove, S. Pollmann, T. Schubert, C. J. Wiggins, D. Y. von Cramon, *Brain Res. Cogn. Brain Res.* **9**, 103 (2000).
23. Y. Nagahama *et al.*, *Cereb. Cortex* **11**, 85 (2001).
24. K. Sakai, R. E. Passingham, *Nature Neurosci.* **6**, 75 (2003).
25. E. Koechlin, G. Basso, P. Pietrini, S. Panzer, J. Grafman, *Nature* **399**, 148 (1999).
26. E. Koechlin, G. Corrado, P. Pietrini, J. Grafman, *Proc. Natl. Acad. Sci. U.S.A.* **97**, 7651 (2000).
27. P. S. Goldman-Rakic, in *Handbook of Physiology, The Nervous System*, F. Plum, V. Moutcastle, Eds. (American Physiological Society, Bethesda, MD, 1987), vol. 5, pp. 373–417.
28. T. Shallice, *From Neuropsychology to Mental Structure* (Cambridge Univ. Press, New York, 1988).
29. A. Baddeley, S. Della Sala, *Philos. Trans. R. Soc. London Ser. B* **351**, 1397 (1996).
30. G. T. Fechner, *Elemente der Psychophysik* (Breitkopf and Härtel, Leipzig, Germany, 1860).
31. K. H. Norwich, W. Wong, *Percept. Psychophys.* **59**, 929 (1997).

32. We thank S. Dehaene, J. Grafman, and E. Guigon for helpful discussions and the Service Hospitalier Frédéric Joliot (Orsay, France) for MRI facilities. Supported by the French Ministry of Research (Action Concertée Incitative grant no. 22-2002-350) and the Institut Fédératif de Recherche d'Imagerie Neurofonctionelle (IFR49).

Supporting Online Material

www.sciencemag.org/cgi/content/full/302/5648/1181/DC1
Materials and Methods
SOM Text
Figs. S1 and S2
Table S1
References

27 June 2003; accepted 30 September 2003

REPORTS

Persistence of Memory in Drop Breakup: The Breakdown of Universality

Pankaj Doshi,[1]* Itai Cohen,[2] Wendy W. Zhang,[3]† Michael Siegel,[4] Peter Howell,[5] Osman A. Basaran,[1] Sidney R. Nagel[3]

A low-viscosity drop breaking apart inside a viscous fluid is encountered when air bubbles, entrained in thick syrup or honey, rise and break apart. Experiments, simulations, and theory show that the breakup under conditions in which the interior viscosity can be neglected produces an exceptional form of singularity. In contrast to previous studies of drop breakup, universality is violated so that the final shape at breakup retains an imprint of the initial and boundary conditions. A finite interior viscosity, no matter how small, cuts off this form of singularity and produces an unexpectedly long and slender thread. If exterior viscosity is large enough, however, the cutoff does not occur because the minimum drop radius reaches subatomic dimensions first.

Underlying one of the common occurrences of daily life, the breakup of a liquid drop, is a rich and beautiful phenomenon. As a drop divides, the neck connecting the different masses of fluid necessarily becomes arbitrarily thin with a curvature that grows without bound until molecular scales are reached. Because surface tension gives rise to a pressure proportional to the curvature, this pressure also diverges. Similar singularities, in which a physical quantity effectively diverges, occur in many different realms, ranging from the subatomic-nuclear fission (*1*) to the celestial-star formation (*2*). The ubiquity, simplicity, and accessibility of drop breakup makes it ideal for studying divergent dynamical behavior that occurs elsewhere in nature.

Near such a singularity, the dynamics are normally governed by the proximity to the singularity, and the dynamics become universal so that all memory of initial and boundary conditions is lost. In such cases, the breakup becomes scale-invariant; after appropriate rescaling, drop shapes near the breakup can be superimposed at different times onto a single form, depending on only a few material parameters (*3*–*6*).

Here, we report an important exception to this class of behavior: the breakup of a zero-viscosity drop inside an extremely viscous exterior fluid produces an unexpected, nonuniversal form of singularity, in which the memory of the initial conditions persists throughout the breakup process. Axial structure imposed at the outset on large length scales remains as the thin neck collapses. The unusual character of this breakup suggests a novel and controllable method for producing submicrometer structures.

Because all classical fluids have a finite viscosity, it is important to understand the nature of the singularity when the interior viscosity is very small but nonzero. If the interior viscosity is sufficiently small, as it is for an air bubble in thick syrup, the zero-viscosity drop breakup dynamics persist down to the atomic scales. However, if the interior viscosity is large enough, or the exterior viscosity small enough, the singularity will be cut off. In this case, the large-scale shape of the drop assumes an unexpected appearance. The smooth profile is transformed into a long and thin thread, which can be less than 1 μm thick. The drop and surrounding fluid in our experiment were chosen to display the zero-viscosity drop breakup dynamics, which remember initial and boundary conditions, and the subsequent destruction of the dynamics by the effect of a finite interior viscosity.

Figure 1 shows a water drop with an interior fluid viscosity $\mu_{int} = 0.01$ poise (1 poise = 1 g cm^{-1} s^{-1}) as it drips through silicone oil (polydimethylsiloxane) with an exterior fluid viscosity of $\mu_{ext} = 120$ poise. The drop shape near the minimum forms a quadratic profile that remains smooth and symmetric about the minimum as the neck collapses radially (Fig. 1, A to C). This quadratic regime, with constant axial curvature, persists until the neck thins to a radius of about 100 μm, at which point the thinning of the neck slows dramatically. The slowing begins at the minimum and propagates axially so that a thin thread is formed connecting the two conical regions of the drop (Fig. 1, D and E). Finally, the drop breaks at the two ends of the thread.

In both experiments and simulations, we investigated the dynamics of the quadratic breakup regime (Fig. 1, A to C) by measuring the radius of the drop profile $h(z, t)$ as a function of z, the axial position measured from the min-

[1]School of Chemical Engineering, Purdue University, West Lafayette, IN 47907, USA. [2]Physics and Division of Engineering and Applied Sciences, Harvard University, Cambridge, MA 02138, USA. [3]The Physics Department and the James Franck Institute, University of Chicago, Chicago, IL 60637, USA. [4]Department of Mathematical Sciences, New Jersey Institute of Technology, Newark, NJ 07102, USA. [5]Mathematical Institute, 24–29 Saint Giles', Oxford OX 13LB, UK.

*Present address: Department of Chemical Engineering, Massachusetts Institute of Technology, Cambridge, MA 02139, USA.
†To whom correspondence should be addressed. E-mail: wzhang@uchicago.edu

The Architecture of Cognitive Control in the Human Prefrontal Cortex

Etienne Koechlin, Chrystèle Ody and Frédérique Kouneiher

Science **302** (5648), 1181-1185.
DOI: 10.1126/science.1088545